ISSN 0081-5438, Proceedings of the Steklov Institute of Mathematics, 2023, Vol. 321, pp. 54–68. © The Author(s) 2023.
This article is an open access publication. Russian Text © The Author(s), 2023, published in Trudy Matematicheskogo Instituta imeni V.A. Steklova, 2023, Vol. 321, pp. 62–76.

# Front Asymptotics of a Flat Sub-Riemannian Structure on the Engel Distribution

**I. A. Bogaevsky** [a,b]

Received March 20, 2022; revised December 14, 2022; accepted February 17, 2023

**Abstract**—We approximate the front of a flat sub-Riemannian structure on the Engel distribution in a neighborhood of a non-subanalytic singularity by the front of a control system integrable in elementary functions. As a corollary, we find the asymptotics of the exponential map of a flat sub-Riemannian structure on the Engel distribution.

**DOI:** 10.1134/S0081543823020049

## 1. INTRODUCTION

The sphere of radius $\tau > 0$ of a flat sub-Riemannian structure on the Engel distribution is a compact singular hypersurface in $\mathbb{R}^4$. It is the boundary of the set reachable from the origin in time $\tau$ for a control system in $\mathbb{R}^4$ whose admissible velocities at every point form a two-dimensional disk:

$$\dot{x} = u_1, \qquad \dot{y} = u_2, \qquad \dot{z} = u_1\frac{y}{2} - u_2\frac{x}{2}, \qquad \dot{w} = u_1\frac{y^2}{2}, \qquad u_1^2 + u_2^2 \le 1. \tag{1.1}$$

In what follows we call this sphere the *Engel sphere*.

The Engel sphere is a subset of the image in $\mathbb{R}^4$ of the exponential map of a three-dimensional cylinder (product of a circle and a plane). The exponential map is analytic; explicit formulas in terms of Jacobi elliptic functions and elliptic integrals for this map were found in [4]. The closure of the image of the exponential map is called the *Engel front*.

The control system (1.1), as well as the Engel sphere and front, are symmetric with respect to the involutions

$$(x, y, z, w) \mapsto (x, -y, -z, w), \qquad (x, y, z, w) \mapsto (-x, -y, z, -w). \tag{1.2}$$

Moreover, the linear transformation

$$(t, x, y, z, w) \mapsto (\tau t, \tau x, \tau y, \tau^2 z, \tau^3 w) \tag{1.3}$$

preserves the control system (1.1) and maps the Engel sphere (front) of unit radius to the Engel sphere (front) of radius $\tau$.

The sphere is not subanalytic at the points $x = \pm\tau$, $y = z = w = 0$ (which we call *poles*). The preimage of each pole under the exponential map is a (noncompact) straight line in the two-dimensional generator of the cylinder.

The absence of subanalyticity at the poles follows from the results of [2], where this is proved for a sphere of a flat sub-Riemannian structure on the Martinet distribution in the three-dimensional space; the latter sphere is the boundary of the projection of the Engel sphere along the $z$ axis.

[a] Faculty of Mechanics and Mathematics, Lomonosov Moscow State University, Moscow, 119991 Russia.

[b] Scientific Research Institute for System Analysis of the Russian Academy of Sciences, Nakhimovskii prosp. 36-1, Moscow, 117218 Russia.

E-mail address: ibogaevsk@gmail.com

Similarly, the boundary of the projection of the Engel sphere along the $w$ axis is a sphere of a flat sub-Riemannian structure on the contact distribution, which was studied in [12]. These facts about the boundaries of the two projections of the Engel sphere are discussed in more detail in Section 3 in terms of the exponential map and the Hamiltonian of the Pontryagin maximum principle.

The Engel sphere was studied in [4–7, 11].

**Results of the study.** In the present paper we analyze a *reduced* control system (2.1), which differs from the original system (1.1) by the narrower set of admissible velocities: instead of the disk $u_1^2 + u_2^2 \le 1$ centered at zero, we consider the set $(2u_1 - 1)^2 + 2u_2^2 \le 1$ bounded by an ellipse with center at the point $u_1 = 1/2$, $u_2 = 0$ and semiaxes $1/2$ and $1/\sqrt{2}$. This ellipse is tangent to the unit circle at the point $u_1 = 1$, $u_2 = 0$ and passes through the point $u_1 = u_2 = 0$.

Recall that the reachable set of a control system consists of points that can be reached along admissible trajectories in time at most $\tau > 0$. According to Filippov's theorem (see [3, Sect. 10.3]) and Krener's theorem (see [3, Sect. 8.1]), the reachable sets of the control systems (1.1) and (2.1) are compact and coincide with the closures of their interiors. The trajectories along which one can reach the boundary of the reachable set from a given point in time $\tau$ are said to be *geometrically optimal*.

The admissible trajectories satisfying the Pontryagin maximum principle for a time-optimal problem are called *extremals*. Any geometrically optimal trajectory is an extremal; the converse is not true in general. The points that can be reached from a given point in time $\tau$ along extremals form a *front*. The front contains all points of the boundary of the reachable set, but, generally speaking, is not exhausted by them.

It turns out that in contrast to the original system (1.1), the extremals of the reduced control system (2.1) can be expressed in terms of elementary functions; therefore, the front $\Phi_\tau$ and the reachable set $\mathcal{A}_\tau$ of this system can be analyzed in great detail. Explicit formulas for the extremals of the reduced control system (2.1) are obtained in Theorem 1, and those for the front $\Phi_\tau$ and the boundary of the reachable set $\partial\mathcal{A}_\tau \subset \Phi_\tau$, in Corollaries 1 and 2.

In Theorem 2, we find the asymptotics of the exponential map in elementary functions at all points of the preimage of the pole $x = 1$, $y = z = w = 0$ of the Engel sphere of unit radius. (Due to the second symmetry in (1.2), it suffices to consider one pole.) Explicit formulas for the exponential map that contain Jacobi elliptic functions and elliptic integrals were found in [4].

Informally speaking, Theorem 3 states that the front of the reduced control system (2.1) touches the Engel front in the neighborhood of the pole $x = \tau$, $y = z = w = 0$. The exact statement of the theorem is explained below. Conjecture 1 strengthens Theorem 3, but remains unproven.

All cross-sections $x = \tau(1 - \varepsilon)$ for $0 < \varepsilon < 1$ of the boundary $\partial\mathcal{A}_\tau$ of the reachable set of the reduced control system (2.1) coincide with a surface $\mathcal{S}$ up to invertible linear transformations preserving the coordinate axes. The surface $\mathcal{S}$ is defined by formulas (2.6) and is depicted in Fig. 1 from two different angles. It is smooth outside the edge that is clearly seen in Fig. 1a. For $\varepsilon = 0$ and 1, the cross-sections under consideration degenerate into the origin.

The surface $\mathcal{S}$ is symmetric with respect to the vertical axis $w$. After the smooth change (2.7) of the coordinate $w$, it becomes symmetric with respect to both vertical coordinate planes, albeit strongly distorted. The resulting transformed surface is shown in Fig. 2 from two different angles. Despite strong distortions, the new coordinates are much more convenient: the surface $\mathcal{S}$ looks much clearer in these coordinates.

All cross-sections $x = \tau(1 - \varepsilon)$ with $0 < \varepsilon < 1$ of the front of the reduced control system coincide with a surface $\mathcal{F}$ up to invertible linear transformations preserving the coordinate axes. The surface $\mathcal{F}$ is defined by formulas (2.5) and consists of the surface $\mathcal{S}$ and the interior, which is difficult to represent in the coordinates $(y, z, w)$. It is better to use again the change (2.7): Figure 3 shows the interior of the transformed surface $\mathcal{F}$ from four different angles (the two top views are from

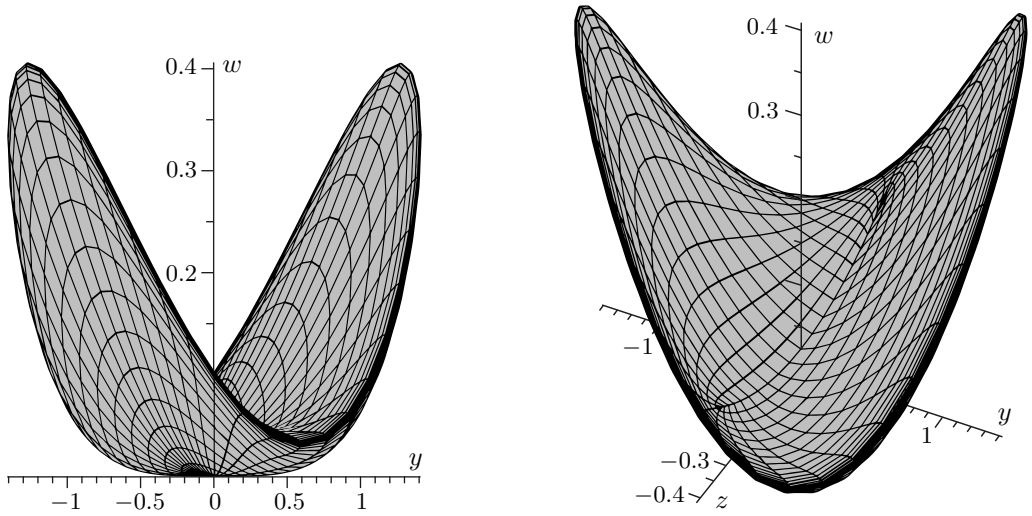


**Fig. 1.** Cross-section of the reachable set of the reduced system.

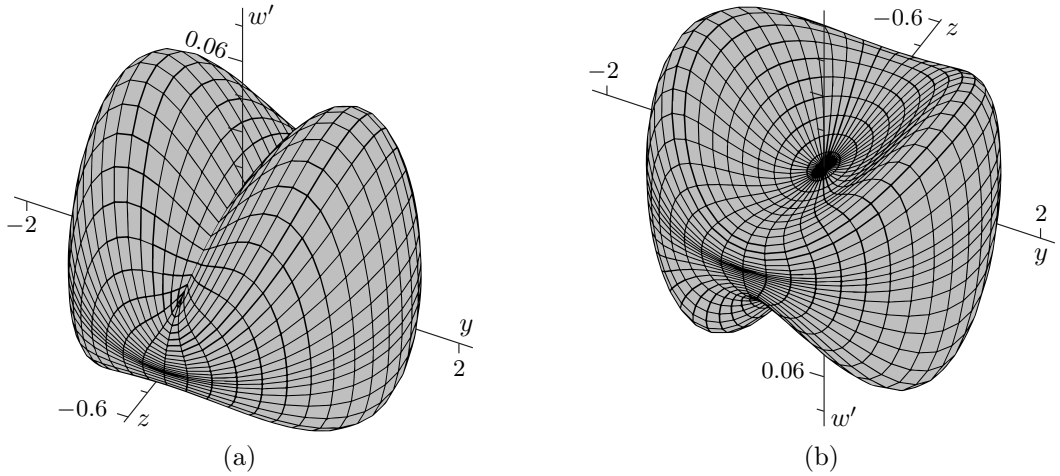


**Fig. 2.** Transformed cross-section of the reachable set.

the same angles as in Fig. 2). Figure 4 demonstrates the upper part (i.e., the part distinguished by the condition $w' \geq 0$ on the new coordinate (2.7)) of the transformed surface $\mathcal{F}$ from two different angles.

The surface $\mathcal{F}$ has a rather complicated structure. Namely, it contains self-intersection edges, cuspidal edges, and swallowtails. These singularities accumulate at the origin. The self-intersection edges lie on the vertical coordinate planes $x = 0$ and $z = 0$ and terminate at the points of swallowtails. The cuspidal edges are of two types: smooth closed curves and astroid-like curves that have semicubic singularities at the points of swallowtails. As we approach the origin, cuspidal edges of different types alternate, although this is difficult to see in the figures because smooth curves lie very close to the astroids.

Informally speaking, the singularities of $\mathcal{F}$ are arranged in the same way as on the front of a typical sub-Riemannian structure on the contact distribution (see [1, 9]).

Theorem 3 and Conjecture 1 state that the surface $\mathcal{F}$ approximates the vertical cross-sections of the Engel front in the following sense. Denote by $\mathcal{F}^{\mathrm{E}}$ the lower limit as $\varepsilon \to 0+$ of the image of the cross-section $x = \tau(1-\varepsilon)$ of the Engel front at time $\tau$ under the quasihomogeneous dilation (4.1). (The lower limit is the set of those points for each of which the distance to the image of the cross-

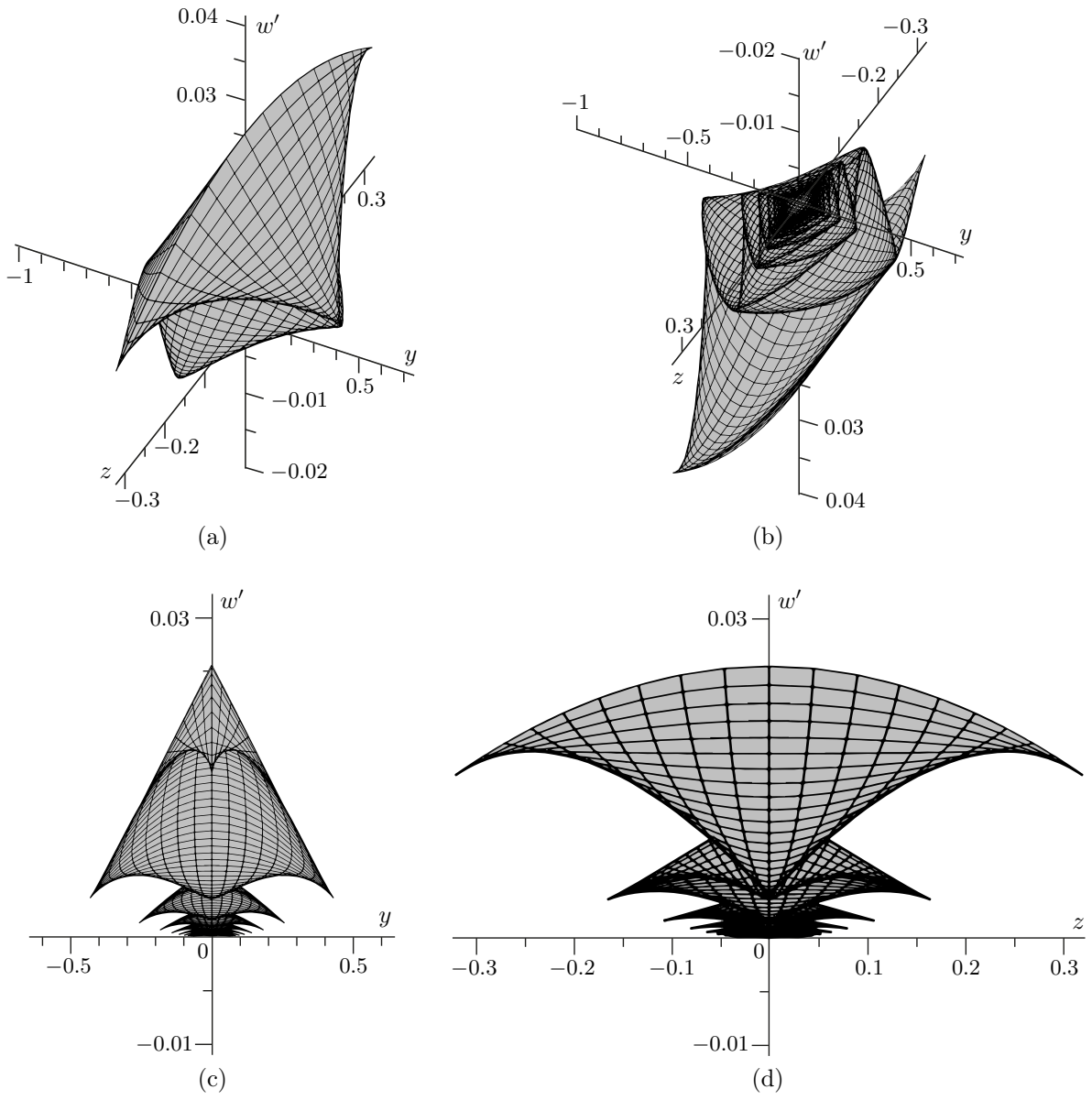


**Fig. 3.** Interior of the transformed cross-section of the front.

section tends to zero as $\varepsilon \to 0+$.) The conjecture states that $\mathcal{F}^{\mathrm{E}} = \mathcal{F}$. To date, this conjecture has not been proved, but, according to Theorem 3, we have $\mathcal{F}^{\mathrm{E}} \supset \mathcal{F}$.

At first glance, the conjecture is false: it is well known that the cross-sections of the Engel sphere and the front have a more complicated structure than the surfaces $\mathcal{S}$ and $\mathcal{F}$, respectively. However, this fact does not disprove our conjecture, which states that passing to the limit simplifies everything. In other words, the complicated part has a higher order of smallness and vanishes in the limit.

In addition, our conjecture is consistent with the results obtained in [8] for the limit cross-sections of the sphere and the front of a flat sub-Riemannian structure on the Martinet distribution. The point is that the Martinet sphere is the boundary of the projection of the Engel sphere along the $z$ axis; therefore, the boundary of the projection of the surface $\mathcal{S}$ (Fig. 1a) is the limit cross-section of the Martinet sphere obtained in [8]. According to the results of [8], in the cross-section of the Martinet front, there is indeed another interior part with singularities, which is not seen in the limit cross-section because it turns into the origin when we pass to the limit.

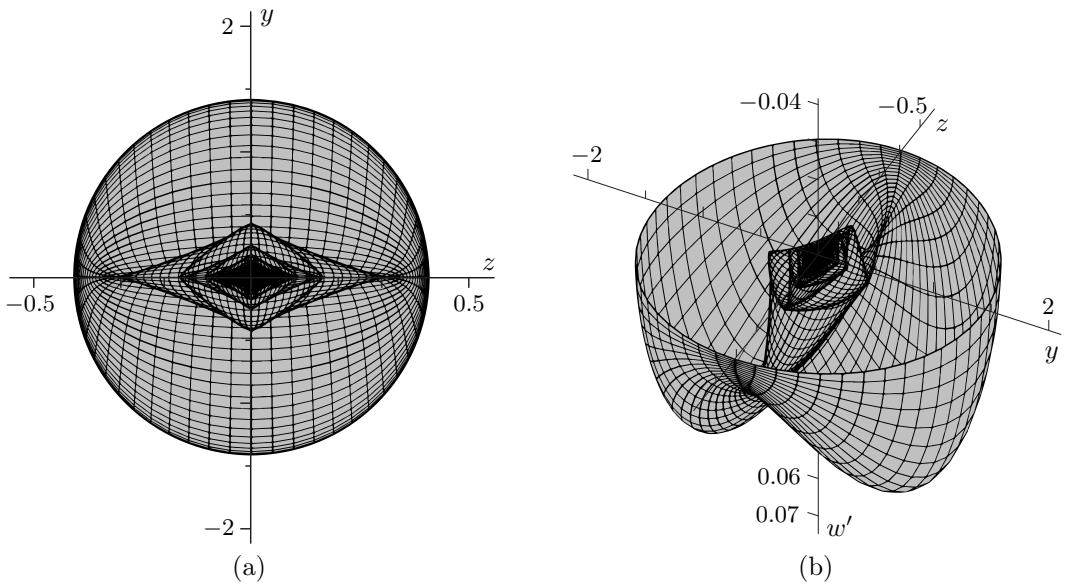


**Fig. 4.** Upper part of the transformed cross-section of the front.

However, a similar conjecture in the Martinet case has not been rigorously proved in [8] either, but the vanishing interior was analyzed and shown to be of higher order of smallness. Most likely a similar phenomenon occurs for the Engel front, and the structure of its cross-section close to the pole is similar to the structure of the front of a typical sub-Riemannian structure on the contact distribution. When we pass to the limit, a half of the cross-section becomes smooth.

**Motivation of the study.** The planes containing the disks of admissible velocities of the control system (1.1) form the Engel distribution generated by the pair of vector fields

$$v_1 = \partial_x + \frac{y}{2}\partial_z + \frac{y^2}{2}\partial_w, \qquad v_2 = \partial_y - \frac{x}{2}\partial_z.$$

According to the Engel theorem, a generic smooth distribution of two-dimensional planes in $\mathbb{R}^4$ in some local coordinates in the neighborhood of almost any point is defined by the vector fields $v_1$ and $v_2$. In this sense, the Engel distribution is universal, just as the contact distribution in $\mathbb{R}^3$.

The integral curves of the vector field $v_1$ are called abnormal geodesics; they are geodesics for any sub-Riemannian metric on the Engel distribution. The sub-Riemannian distance has very complicated and mysterious singularities along abnormal geodesics.

There are many sub-Riemannian structures on the Engel distribution that are not equivalent to each other with respect to changes of smooth local coordinates; just as Riemannian structures, they differ in functional invariants. Nevertheless, all of them have isometric tangent spaces in the Gromov–Hausdorff sense (see [10] for details). This tangent space is called a flat sub-Riemannian structure on the Engel distribution; it is the sphere and the front of this structure for which we analyze the asymptotics near abnormal geodesics in this paper, since the poles of the Engel sphere are precisely the points of its intersection with abnormal geodesics emanating from the center of the sphere.

## 2. FRONT OF THE REDUCED CONTROL SYSTEM

In this section, we present formulas for the extremals, for the boundary of the reachable set, and for the front of the *reduced* control system

$$\dot{x} = u_1, \qquad \dot{y} = u_2, \qquad \dot{z} = u_1\frac{y}{2} - u_2\frac{x}{2}, \qquad \dot{w} = u_1\frac{y^2}{2}, \qquad (2u_1 - 1)^2 + 2u_2^2 \le 1, \qquad (2.1)$$

which differs from the original system (1.1) in that it has a narrower set of admissible velocities: instead of the disk $u_1^2+u_2^2\le 1$ centered at zero, we consider a set bounded by an ellipse with center at the point $u_1=1/2$, $u_2=0$ and semiaxes $1/2$ and $1/\sqrt{2}$. This ellipse is tangent to the unit circle at the point $u_1=1$, $u_2=0$. It turns out that in contrast to the original system (1.1), the extremals of the reduced control system can be expressed in terms of elementary functions.

Introduce the notation

$$\gamma_\beta=1-\frac{\beta}{3!}+\frac{\beta^2}{5!}-\frac{\beta^3}{7!}+\ldots=\frac{\sin\sqrt{\beta}}{\sqrt{\beta}}=\frac{\sinh\sqrt{-\beta}}{\sqrt{-\beta}},$$

$$\delta_\beta=1-\frac{\beta}{2!}+\frac{\beta^2}{4!}-\frac{\beta^3}{6!}+\ldots=\cos\sqrt{\beta}=\cosh\sqrt{-\beta}$$

for analytic functions of the parameter $\beta$.

**Theorem 1.** *The space–time curves defined in the coordinates $t,x,y,z,w$ by the equations*

$$t=x+xT^{(2)}_{\alpha x^2}(\theta,cx),\qquad y=xY^{(1)}_{\alpha x^2}(\theta,cx),\qquad z=x^2Z^{(1)}_{\alpha x^2}(\theta,cx),\qquad w=x^3W^{(2)}_{\alpha x^2}(\theta,cx),\tag{2.2}$$

*with parameters $\theta,c,\alpha\in\mathbb{R}$, are extremals of the reduced control system (2.1) that emanate from the origin. Here*

$$T^{(2)}_\beta(\theta,b)=\theta^2\frac{\gamma_\beta\delta_\beta+1}{4}-\theta b\frac{\gamma_\beta^2}{2}+b^2\frac{1-\gamma_\beta\delta_\beta}{4\beta},\qquad T^{(2)}_0(\theta,b)=\frac{\theta^2}{2}-\frac{\theta b}{2}+\frac{b^2}{6},$$

$$Y^{(1)}_\beta(\theta,b)=\theta\gamma_\beta+b\frac{\delta_\beta-1}{\beta},\qquad Y^{(1)}_0(\theta,b)=\theta-\frac{b}{2},$$

$$Z^{(1)}_\beta(\theta,b)=\theta\left(\frac{1-\delta_\beta}{\beta}-\frac{\gamma_\beta}{2}\right)+b\frac{2\gamma_\beta-\delta_\beta-1}{2\beta},\qquad Z^{(1)}_0(\theta,b)=\frac{b}{12},$$

$$W^{(2)}_\beta(\theta,b)=\theta^2\frac{1-\gamma_\beta\delta_\beta}{4\beta}-\theta b\frac{(1-\delta_\beta)^2}{2\beta^2}+b^2\frac{\gamma_\beta\delta_\beta-4\gamma_\beta+3}{4\beta^2},\qquad W^{(2)}_0(\theta,b)=\frac{\theta^2}{6}-\frac{\theta b}{8}+\frac{b^2}{40}$$

*are homogeneous polynomials in $(\theta,b)$ with coefficients analytically depending on $\beta$ whose degrees are indicated in parentheses.*

*Moreover, the admissible trajectories of the form*

$$x=\varphi(t),\qquad y=z=w=0,\qquad \varphi\in C(\mathbb{R}),\quad \varphi(0)=0,\quad 0\le\dot\varphi(t)\le 1,\tag{2.3}$$

*where the last condition holds for almost all $t\in\mathbb{R}$, are also extremals emanating from the origin.*

*The reduced control system (2.1) has no other nonextendable extremals.*

**Remark 1.** The extremals (2.2) are the projections of the solutions of the Hamilton equations with the Hamiltonian $H$ (5.1) defined by the Pontryagin maximum principle. On the extremals (2.3), the Hamiltonian $H$ loses its smoothness; therefore, these extremals are said to be *singular*. It is interesting that all singular extremals (2.3) of the reduced control system (2.1) are geometrically optimal. This observation follows immediately from Corollary 2 to Theorem 1.

**Corollary 1.** *The front $\Phi_\tau$ of the reduced control system (2.1) is the closure of the three-dimensional singular hypersurface*

$$\Phi^\circ_\tau=\Big\{y=\sqrt{x(\tau-x)}\mathcal{Y}(\beta)\cos\psi,\ z=\sqrt{x^3(\tau-x)}\mathcal{Z}(\beta)\sin\psi,\\ w=x^2(\tau-x)\big(\mathcal{W}_0(\beta)\cos^2\psi+\mathcal{W}_1(\beta)\cos\psi\sin\psi+\mathcal{W}_2(\beta)\sin^2\psi\big)\Big\}\tag{2.4}$$

*defined by equations with parameters* $\psi \in \mathbb{R}/2\pi\mathbb{Z}$ *and* $\beta \in \mathbb{R}$, *where*

$$\mathcal{Y}(\beta) = \frac{2\gamma_{\beta/4}}{\sqrt{1+\gamma_\beta}}, \qquad \mathcal{Z}(\beta) = \frac{2(\gamma_{\beta/4} - \delta_{\beta/4})}{\beta}\sqrt{\frac{\beta}{1-\gamma_\beta}}, \qquad \mathcal{W}_0(\beta) = \frac{2-\gamma_\beta-\delta_\beta}{\beta(1+\gamma_\beta)},$$
$$\mathcal{W}_1(\beta) = \frac{2(2-\beta\gamma_\beta-2\delta_\beta)}{\beta^2}\sqrt{\frac{\beta}{1-\gamma_\beta^2}}, \qquad \mathcal{W}_2(\beta) = \frac{2-3\gamma_\beta+\delta_\beta}{\beta(1-\gamma_\beta)}$$

*are analytic functions of* $\beta$ *with*

$$\mathcal{Y}(0) = \sqrt{2}, \qquad \mathcal{Z}(0) = \frac{1}{\sqrt{6}}, \qquad \mathcal{W}_0(0) = \frac{1}{3}, \qquad \mathcal{W}_1(0) = \frac{1}{2\sqrt{3}}, \qquad \mathcal{W}_2(0) = \frac{1}{10}.$$

*The complement* $\Phi_\tau \setminus \Phi_\tau^\circ$ *is the interval* $0 < x < \tau$ *of the abscissa.*

**Remark 2.** The hypersurface $\Phi_\tau^\circ$ can also be defined by the equations

$$y = \sqrt{x(\tau-x)}\,Y_\beta^{(0)}(\theta,b), \qquad z = \sqrt{x^3(\tau-x)}\,Z_\beta^{(0)}(\theta,b), \qquad w = x^2(\tau-x)W_\beta^{(0)}(\theta,b)$$

with parameters $\theta, b, \beta \in \mathbb{R}$, where

$$Y_\beta^{(0)}(\theta,b) = \frac{Y_\beta^{(1)}(\theta,b)}{\sqrt{T_\beta^{(2)}(\theta,b)}}, \qquad Z_\beta^{(0)}(\theta,b) = \frac{Z_\beta^{(1)}(\theta,b)}{\sqrt{T_\beta^{(2)}(\theta,b)}}, \qquad W_\beta^{(0)}(\theta,b) = \frac{W_\beta^{(2)}(\theta,b)}{T_\beta^{(2)}(\theta,b)}$$

are analytic functions defined for $(\theta,b) \neq 0$ that do not change under the homogeneous dilations $(\theta,b) \mapsto (\lambda\theta,\lambda b)$ with $\lambda > 0$.

**Corollary 2.** *The boundary* $\partial\mathcal{A}_\tau \subset \Phi_\tau$ *of the reachable set of the reduced control system* (2.1) *is the complement of the interior of the front* $\Phi_\tau$ *to the whole* $\Phi_\tau$; *this interior is distinguished from the hypersurface* $\Phi_\tau^\circ$ *by the condition* $\beta > 4\pi^2$.

All cross-sections of the fronts $\Phi_\tau$ by the hyperplanes $x = \tau(1-\varepsilon)$, where $\tau > 0$ and $0 < \varepsilon < 1$, coincide, up to linear transformations preserving the $y$, $z$, and $w$ coordinate axes, with the surface

$$\mathcal{F} = \Big\{ y = \mathcal{Y}(\beta)\cos\psi,\ z = \mathcal{Z}(\beta)\sin\psi,$$
$$w = \mathcal{W}_0(\beta)\cos^2\psi + \mathcal{W}_1(\beta)\cos\psi\sin\psi + \mathcal{W}_2(\beta)\sin^2\psi \ \Big|\ \psi \in \mathbb{R}/2\pi\mathbb{Z},\ \beta \in \mathbb{R}\Big\} \cup O, \quad (2.5)$$

which lies in $\mathbb{R}^3 = \{(y,z,w)\}$; here $O = (0,0,0)$.

Similarly, all cross-sections of the boundaries $\partial\mathcal{A}_\tau$ by the hyperplanes $x = \tau(1-\varepsilon)$, where $\tau > 0$ and $0 < \varepsilon < 1$, coincide, up to linear transformations preserving the $y$, $z$, and $w$ coordinate axes, with the surface $\mathcal{S} \subset \mathcal{F}$,

$$\mathcal{S} = \Big\{ y = \mathcal{Y}(\beta)\cos\psi,\ z = \mathcal{Z}(\beta)\sin\psi,$$
$$w = \mathcal{W}_0(\beta)\cos^2\psi + \mathcal{W}_1(\beta)\cos\psi\sin\psi + \mathcal{W}_2(\beta)\sin^2\psi \ \Big|\ \psi \in \mathbb{R}/2\pi\mathbb{Z},\ \beta \le 4\pi^2\Big\} \cup O, \quad (2.6)$$

obtained by removing the interior, defined by the condition $\beta > 4\pi^2$, from the surface $\mathcal{F}$.

**Remark 3.** The projection of the cross-section $\beta = \beta_0$ of the surface $\mathcal{F}$ along the $w$ axis is an ellipse if $\mathcal{Y}(\beta_0) \neq 0$ and $\mathcal{Z}(\beta_0) \neq 0$. This condition is satisfied for all $\beta_0 < 4\pi^2$. For $\beta_0 = 4\pi^2$, the ellipse turns into a line segment since $\mathcal{Y}(4\pi^2) = 0$ and $\mathcal{Z}(4\pi^2) \neq 0$.

**Remark 4.** To analyze the surface $\mathcal{F}$, it is convenient to pass from $w$ to the coordinate

$$w' = w - \frac{y^2}{6} - \frac{yz}{2} - \frac{3z^2}{5}, \quad (2.7)$$

in which the formula for $\mathcal{F}$ is simpler:

$$w' = \mathcal{W}_0'(\beta)\cos^2\psi + \mathcal{W}_2'(\beta)\sin^2\psi, \tag{2.8}$$

where

$$\mathcal{W}_0'(\beta) = \frac{2-3\gamma_\beta+\delta_\beta}{3\beta(1+\gamma_\beta)}, \qquad \mathcal{W}_2'(\beta) = \frac{\beta(4+9\gamma_\beta-\delta_\beta)-24(1-\delta_\beta)}{5\beta^2(1-\gamma_\beta)},$$

with $\mathcal{W}_0'(0) = \mathcal{W}_2'(0) = 0$.

## 3. EXPONENTIAL MAP AND ITS ASYMPTOTICS

The exponential map (in unit time) for the control system (1.1) is constructed as follows. Consider the Hamiltonian

$$H^{\mathrm{E}} = \max_{u_1^2+u_2^2\le 1}(u_1P+u_2Q) = \sqrt{P^2+Q^2}, \qquad P = p_x + p_z\frac{y}{2} + p_w\frac{y^2}{2}, \quad Q = p_y - p_z\frac{x}{2}, \tag{3.1}$$

defined by the Pontryagin maximum principle applied to the system, and introduce a three-dimensional cylinder lying on the hypersurface $\{H^{\mathrm{E}}=1\}$,

$$C = \left\{p_x^2+p_y^2 = 1,\ x=y=z=w=0\right\} \subset T^*\mathbb{R}^4,$$

with an angular coordinate $\theta \in \mathbb{R}/2\pi\mathbb{Z}$ and coordinates $c, \alpha \in \mathbb{R}$ on the generators:

$$p_x = \cos\theta, \qquad p_y = \sin\theta, \qquad p_z = c, \qquad p_w = \alpha.$$

For every initial momentum on the cylinder $C$, consider the corresponding trajectory of the Hamilton equations with Hamiltonian $H^{\mathrm{E}}$. By definition, the exponential map

$$\mathrm{Exp}\colon C \to \mathbb{R}^4$$

sends the initial momentum on $C$ to a point in $\mathbb{R}^4$ through which this trajectory passes at time $t=1$.

The Engel front at time $\tau = 1$ is the closure of the image of the exponential map Exp, and the sub-Riemannian sphere of unit radius is a subset of the front. Explicit formulas for the exponential map in terms of the Jacobi elliptic functions and elliptic integrals were found in [4].

The hyperplane $p_z = 0$ consists of phase curves of the Hamiltonian vector field, because the momentum $p_z$ is a first integral of this field. If we restrict the exponential map Exp to the two-dimensional cylinder $C \cap \{p_z = 0\}$ with coordinates $(\theta, \alpha)$ and then project it to $\mathbb{R}^3$ along the $z$ coordinate, we obtain the exponential map of the control system

$$\dot x = u_1, \qquad \dot y = u_2, \qquad \dot w = u_1\frac{y^2}{2}, \qquad u_1^2+u_2^2 \le 1;$$

the boundary of the reachable set of this system is a sphere of the flat sub-Riemannian structure on the Martinet distribution, which was studied in [2, 8].

The hyperplane $p_w = 0$ also consists of phase curves of the Hamiltonian vector field, because the momentum $p_w$ is a first integral of the field as well. If we restrict the exponential map Exp to the two-dimensional cylinder $C \cap \{p_w = 0\}$ with coordinates $(\theta, c)$ and then project it to $\mathbb{R}^3$ along the $w$ coordinate, we obtain the exponential map of the control system

$$\dot x = u_1, \qquad \dot y = u_2, \qquad \dot z = u_1\frac{y}{2} - u_2\frac{x}{2}, \qquad u_1^2+u_2^2 \le 1;$$

the boundary of the reachable set of this system is a sphere of the flat sub-Riemannian structure on the contact distribution, which was studied in [12].

The preimage of the pole $x=1$, $y=z=w=0$ under the exponential map is the straight line $\theta=0$, $c=0$ in the generator of the cylinder, and the preimage of the pole $x=-1$, $y=z=w=0$ is the straight line $\theta=\pi$, $c=0$.

The exponential map is invariant under the involutions

$$\begin{aligned}&(\theta,c,\alpha)\mapsto(-\theta,-c,\alpha), && (x,y,z,w)\mapsto(x,-y,-z,w),\\ &(\theta,c,\alpha)\mapsto(\theta+\pi,c,-\alpha), && (x,y,z,w)\mapsto(-x,-y,z,-w).\end{aligned}\tag{3.2}$$

In particular, when expressed in coordinates,

$$E(\theta,c,\alpha)=\big(X_\alpha(\theta,c),Y_\alpha(\theta,c),Z_\alpha(\theta,c),W_\alpha(\theta,c)\big)\in\mathbb{R}^4,$$

$Y_\alpha$ and $Z_\alpha$ turn out to be odd functions with respect to the involution $(\theta,c)\mapsto(-\theta,-c)$, while $X_\alpha$ and $W_\alpha$, even functions.

**Theorem 2.** *As $(\theta,c)\to 0$ for a fixed parameter $\alpha$, the following asymptotic expansions hold*:

$$\begin{aligned}&X_\alpha(\theta,c)=1-T^{(2)}_\alpha(\theta,c)+O(r^4), && Y_\alpha(\theta,c)=Y^{(1)}_\alpha(\theta,c)+O(r^3),\\ &Z_\alpha(\theta,c)=Z^{(1)}_\alpha(\theta,c)+O(r^3), && W_\alpha(\theta,c)=W^{(2)}_\alpha(\theta,c)+O(r^4),\end{aligned}$$

*where $r=\sqrt{\theta^2+c^2}$ and the $O$-constants depend on $\alpha$.*

## 4. ASYMPTOTICS OF THE ENGEL FRONT AND SPHERE NEAR THE POLE

In this section we formulate Theorem 3 and Conjecture 1, which state that the front of the reduced control system (2.1) approximates the Engel front near its pole $x=\tau$, $y=z=w=0$.

Denote by $\mathcal{F}^{\mathrm{E}}$ the lower limit as $\varepsilon\to 0+$ of the image of the cross-section of the Engel front at time $\tau$ by the hyperplane $x=\tau(1-\varepsilon)$ under the quasihomogeneous dilation

$$(y,z,w)\mapsto\left(\frac{y}{\tau\sqrt{\varepsilon}},\frac{z}{\tau^2\sqrt{\varepsilon}},\frac{w}{\tau^3\varepsilon}\right).\tag{4.1}$$

The lower limit is the set of those points for each of which the distance to the image of the cross-section tends to zero as $\varepsilon\to 0+$.

**Remark 5.** According to Corollary 1 to Theorem 1, a similar construction for the reduced control system (2.1) gives the surface $\mathcal{F}$. Namely, the lower limit as $\varepsilon\to 0+$ of the image of the cross-section of the front $\Phi_\tau$ by the hyperplane $x=\tau(1-\varepsilon)$ under the quasihomogeneous dilation (4.1) coincides with the surface $\mathcal{F}$.

**Theorem 3.** $\mathcal{F}^{\mathrm{E}}\supset\mathcal{F}$.

**Conjecture 1.** $\mathcal{F}^{\mathrm{E}}=\mathcal{F}$.

## 5. PROOFS

**Proof of Theorem 1.** The Pontryagin maximum principle applied to the reduced control system (2.1) yields the following Hamiltonian, which is homogeneous in the momenta:

$$\begin{aligned}H&=\max_{(2u_1-1)^2+2u_2^2\le 1}(u_1P+u_2Q)=\frac{P+\sqrt{P^2+2Q^2}}{2},\\ P&=p_x+p_z\frac{y}{2}+p_w\frac{y^2}{2},\qquad Q=p_y-p_z\frac{x}{2}.\end{aligned}\tag{5.1}$$

This function is nonnegative and smooth for $(P,Q) \neq (0,0)$. The projections of the solutions of the corresponding Hamilton equations to the configuration space are extremals of the reduced system (2.1).

First, we consider the solutions lying at the level $H = 1$. This is a smooth hypersurface in $T^*\mathbb{R}^4$ defined by the equation $P = 1 - Q^2/2$. At all points of the hypersurface, we have

$$\frac{\partial H}{\partial P} = \frac{1}{1+Q^2/2}, \qquad \frac{\partial H}{\partial Q} = \frac{Q}{1+Q^2/2}.$$

Using these relations, we write down the Hamilton equations with the coordinate $x$ as an independent variable:

$$\frac{dt}{dx} = 1 + \frac{Q^2}{2}, \qquad \frac{dy}{dx} = Q, \qquad \frac{dz}{dx} = -\frac{xQ}{2} + \frac{y}{2}, \qquad \frac{dw}{dx} = \frac{y^2}{2},$$
$$\frac{dp_x}{dx} = \frac{p_z Q}{2}, \qquad \frac{dp_y}{dx} = -\Big(\frac{p_z}{2} + p_w y\Big), \qquad \frac{dp_z}{dx} = 0, \qquad \frac{dp_w}{dx} = 0.$$

The solutions of these equations with the initial conditions

$$t = x = y = z = w = 0, \qquad p_x = 1 - \frac{\theta^2}{2}, \qquad p_y = \theta, \qquad p_z = c, \qquad p_w = \alpha \tag{5.2}$$

are given by formulas (2.2) (we omit the tedious verification of this fact).

If $H = 0$, then $P \leq 0$ and $Q = 0$. At the points with $P < 0$ and $Q = 0$, the Hamilton equations

$$\dot{x} = \dot{y} = \dot{z} = \dot{w} = \dot{p}_x = \dot{p}_y = \dot{p}_z = \dot{p}_w = 0$$

become trivial and yield extremals of the form (2.3) with $\varphi \equiv 0$.

It remains to consider the case $P = Q = 0$. In this case the Hamiltonian is not smooth, and the maximum principle for the reduced control system (2.1) yields the following equations for the momenta:

$$\dot{p}_x = \frac{u_2 p_z}{2}, \qquad \dot{p}_y = -u_1\Big(\frac{p_z}{2} + p_w y\Big), \qquad \dot{p}_z = 0, \qquad \dot{p}_w = 0.$$

Taking into account (2.1), we obtain

$$\dot{P} = u_2(p_z + p_w y) = 0, \qquad \dot{Q} = -u_1(p_z + p_w y) = 0.$$

For $u_1 = u_2 = 0$, we again obtain an extremal of the form (2.3) with $\varphi \equiv 0$. Let

$$p_z + p_w y = 0, \tag{5.3}$$

which, together with the expressions (5.1) for $P$ and $Q$, yields the initial conditions

$$p_x(0) = p_y(0) = p_z(0) = 0, \qquad p_w(0) \neq 0.$$

(The last condition follows from the maximum principle.) Hence, $p_z = 0$ and $p_w = \text{const} \neq 0$, since $\dot{p}_z = \dot{p}_w = 0$. Therefore, (5.3) implies the equality $y = 0$. From conditions (2.1) we conclude that all extremals along which $P = Q = 0$ have the form (2.3). $\square$

**Proof of Corollary 1.** The front consists of the ends of the extremals described in Theorem 1. Changing the parameters in formulas (2.2),

$$\theta = \xi\delta_{\beta/4} + \eta\frac{\gamma_{\beta/4}}{2}, \qquad c = -\xi\frac{\beta\gamma_{\beta/4}}{2x} + \eta\frac{\delta_{\beta/4}}{x}, \qquad \alpha = \frac{\beta}{x^2},$$

we obtain

$$t = x + x\xi^2\frac{1+\gamma_\beta}{4} + x\eta^2\frac{1-\gamma_\beta}{4\beta}, \qquad y = x\xi\gamma_{\beta/4}, \qquad z = x^2\eta\frac{\gamma_{\beta/4}-\delta_{\beta/4}}{\beta},$$
$$w = x^3\xi^2\frac{2-\gamma_\beta-\delta_\beta}{4\beta} + x^3\xi\eta\frac{2-\beta\gamma_\beta-2\delta_\beta}{2\beta^2} + x^3\eta^2\frac{2-3\gamma_\beta+\delta_\beta}{4\beta^2}.$$

The coefficients $1+\gamma_\beta$ and $(1-\gamma_\beta)/\beta$ in the equation $t=\tau$ are positive analytic functions of the parameter $\beta\in\mathbb{R}$, and the formulas

$$\xi = 2\sqrt{\frac{\tau-x}{x(1+\gamma_\beta)}}\cos\psi, \qquad \eta = 2\sqrt{\frac{(\tau-x)\beta}{x(1-\gamma_\beta)}}\sin\psi$$

parameterize the solutions of the equation $t=\tau$. Substituting them into the expressions for $y$, $z$, and $w$, we obtain all points of the hypersurface $\Phi_\tau^\circ$ except the origin $x=y=z=w=0$, which belongs to the front $\Phi_\tau$ since it is the endpoint of the extremal of the form (2.3) with $\varphi\equiv 0$. Thus, $\Phi_\tau^\circ\subset\Phi_\tau$.

The functions $\mathcal{Y}$, $\mathcal{Z}$, $\mathcal{W}_0$, $\mathcal{W}_1$, and $\mathcal{W}_2$ tend to zero as $\beta\to\infty$. Therefore, the closure of the hypersurface $\Phi_\tau^\circ$ also contains the interval $0<x<\tau$ of the abscissa, whose endpoints belong to $\Phi_\tau^\circ$. However, all extremals of the form (2.3) end precisely at the points of the interval $0\le x\le\tau$ of the abscissa. □

**Proof of Corollary 2.** In the front $\Phi_\tau$, consider the complement $\Sigma_\tau$ of its part distinguished from $\Phi_\tau^\circ$ by the condition $\beta>4\pi^2$. Let us prove that $\partial\mathcal{A}_\tau=\Sigma_\tau$.

The coefficients of the first powers of $\theta$ in the expressions for $T^{(2)}_{4\pi^2}$, $Y^{(1)}_{4\pi^2}$, $Z^{(1)}_{4\pi^2}$, and $W^{(2)}_{4\pi^2}$ in Theorem 1 vanish. Therefore, the trajectories (2.2) with opposite values of $\theta$ intersect each other if $x^2=4\pi^2/\alpha$. Hence, no trajectory with $\theta\ne 0$ and $\alpha>0$ is geometrically optimal for $x^2>4\pi^2/\alpha$.

The function $Y^{(1)}_\beta(\theta,b)$ from Theorem 1 and all three of its first derivatives vanish if $\beta=4\pi^2$ and $\theta=0$. Hence, the derivatives of the coordinate $y=xY^{(1)}_{\alpha x^2}(\theta,cx)$ of a point on the trajectory (2.2) with respect to $x$, $\alpha$, $\theta$, and $c$ vanish for $\alpha>0$, $\theta=0$, and $x=x_\alpha$. Therefore, for $x^2=4\pi^2/\alpha$, the point on the trajectory with $\theta=0$ and $\alpha>0$ is conjugate to the origin, and the trajectory in question is not geometrically optimal for $x^2>4\pi^2/\alpha$.

Thus, all trajectories with $\alpha>0$ are not geometrically optimal for $x^2>4\pi^2/\alpha$. Since $\beta=\alpha x^2$, this last condition is nothing else but $\beta>4\pi^2$. Therefore, $\partial\mathcal{A}_\tau\subset\Sigma_\tau$, and the complement $\Phi_\tau\setminus\Sigma_\tau$ is contained in the interior of the reachable set $\mathcal{A}_\tau$.

The following idea was communicated to the author by L. V. Lokutsievskiy. By Filippov's theorem (see [3, Sect. 10.3]) and Krener's theorem (see [3, Sect. 8.1]), the reachable set $\mathcal{A}_\tau$ is compact and is the closure of its interior. Therefore, its boundary $\partial\mathcal{A}_\tau$ divides $\mathbb{R}^4$ into two (or more) connected components. However, no proper subset of $\Sigma_\tau$ has such a property, as demonstrated below. Hence, $\partial\mathcal{A}_\tau=\Sigma_\tau$.

Let us show that the complement of any proper subset of $\Sigma_\tau$ to $\mathbb{R}^4$ is connected.

First, we notice that the surface $\mathcal{S}$ defined by (2.6) is the union of the graphs $w=s_\pm(y,z)$ of two continuous functions $s_\pm$ defined on the disk $y^2+z^2\le 1$. These functions coincide on the circle $y^2+z^2=1$, while for $y^2+z^2<1$ the inequality $s_-(y,z)<s_+(y,z)$ holds. It is more convenient to prove the statement by passing to the coordinate $w'$ defined by formula (2.7) in Remark 4; the validity of the statement is confirmed by Fig. 2. The formal argument is as follows.

In the interval $[0,4\pi^2]$, the functions $\mathcal{Y}$ and $\mathcal{Z}$ are strictly decreasing, with $\mathcal{Y}(0)=\mathcal{Z}(0)=1$, $\mathcal{Y}(4\pi^2)=0$, and $\mathcal{Z}(4\pi^2)>0$. Therefore, a unique ellipse $y=\mathcal{Y}(\beta)\cos\psi$, $z=\mathcal{Z}(\beta)\sin\psi$ with $\beta\in[0,4\pi^2]$ passes through any point of the disk $y^2+z^2\le 1$. Substituting the corresponding values of the parameters $\beta$ and $\psi$ into (2.8), we obtain the value of the function $s'_+(y,z)$. This function

is continuous in the disk $y^2+z^2\le 1$, vanishes on its boundary, since $\mathcal{W}_0'(0)=\mathcal{W}_2'(0)=0$, and is positive in its interior, since $\mathcal{W}_0'(\beta)>0$ and $\mathcal{W}_2'(\beta)>0$ if $\beta>0$.

On the ray $(-\infty,0]$, the functions $\mathcal{Y}$ and $\mathcal{Z}$ are strictly increasing, tend to zero as $\beta\to-\infty$, and $\mathcal{Y}(0)=\mathcal{Z}(0)=1$. Therefore, a unique ellipse $y=\mathcal{Y}(\beta)\cos\psi$, $z=\mathcal{Z}(\beta)\sin\psi$ with $\beta\in(-\infty,0]$ passes through any point of the punctured disk $0<y^2+z^2\le 1$. Substituting the corresponding values of the parameters $\beta$ and $\psi$ into (2.8), we obtain the value of the function $s'_-(y,z)$. In addition, let $s'_-(0,0)=0$. The function $s_-$ is continuous in the disk $y^2+z^2\le 1$, since $\mathcal{W}_0$ and $\mathcal{W}_2$ tend to zero as $\beta\to-\infty$. The function $s_-$ vanishes on the circle $x^2+y^2=1$, since $\mathcal{W}_0'(0)=\mathcal{W}_2'(0)=0$, and is negative in the punctured disk $0<y^2+z^2<1$, since $\mathcal{W}_0'(\beta)<0$ and $\mathcal{W}_2'(\beta)<0$ if $\beta<0$.

When we pass from the coordinate $w'$ to the coordinate $w$, the graphs $w'=s'_\pm(y,z)$ of the functions $s'_\pm$ transform into the graphs $w=s_\pm(y,z)$ of the functions $s_\pm$ with the above properties. By Corollary 1, the cross-section of the hypersurface $\Sigma_\tau$ by the vertical hyperplane $x=\text{const}$ is obtained from the surface $\mathcal{S}$ by the linear transformation

$$(y,z,w)\mapsto\big(\sqrt{x(\tau-x)}y,\sqrt{x^3(\tau-x)}z,\,x^2(\tau-x)w\big).$$

Hence, the hypersurface $\Sigma_\tau$ is the union of the graphs $w=\sigma_\pm(x,y,z)$ of two continuous functions $\sigma_\pm$ defined on the closure of the connected bounded domain

$$U=\left\{\frac{y^2}{x(\tau-x)}+\frac{z^2}{x^3(\tau-x)}<1,\ 0<x<\tau\right\}$$

by the formulas

$$\sigma_\pm(x,y,z)=x^2(\tau-x)\,s_\pm\left(\frac{y}{\sqrt{x(\tau-x)}},\frac{z}{\sqrt{x^3(\tau-x)}}\right),\qquad \sigma_\pm(0,0,0)=0.$$

These functions coincide on the boundary of the domain $U$, while in the domain itself the inequality $\sigma_-(x,y,z)<\sigma_+(x,y,z)$ holds. Therefore, the complement of any proper subset of $\Sigma_\tau$ to $\mathbb{R}^4$ is connected. $\square$

**Proof of the formulas in Remark 2.** The functions $Y_\beta^{(0)}$, $Z_\beta^{(0)}$, and $W_\beta^{(0)}$ are defined for $(\theta,b)\ne 0$, since $T_\beta^{(2)}$ is a positive definite quadratic form for all $\beta\in\mathbb{R}$, which follows from its explicit formula given in Theorem 1.

Making the change of parameters $b=cx$ and $\beta=\alpha x^2$ in (2.2), we obtain

$$t=x+xT_\beta^{(2)}(\theta,b),\qquad y=xY_\beta^{(1)}(\theta,b),\qquad z=x^2Z_\beta^{(1)}(\theta,b),\qquad w=x^3W_\beta^{(2)}(\theta,b).\tag{5.4}$$

Let $\tau>x>0$ and $(\theta_*,b_*)\ne 0$. For any $\beta\in\mathbb{R}$, the equation

$$\tau=x+xT_\beta^{(2)}(\lambda\theta_*,\lambda b_*)$$

has a unique positive root

$$\lambda=\sqrt{\frac{\tau-x}{xT_\beta^{(2)}(\theta_*,b_*)}},$$

since $T_\beta^{(2)}(\lambda\theta_*,\lambda b_*)=\lambda^2T_\beta^{(2)}(\theta_*,b_*)$. The substitution of $\theta=\lambda\theta_*$ and $b=\lambda b_*$ into formulas (5.4) yields a point in $\Phi_\tau$, and its coordinates satisfy the relations of Corollary 1 for $\theta=\theta_*$ and $b=b_*$, because

$$Y_\beta^{(1)}(\lambda\theta_*,\lambda b_*)=\lambda Y_\beta^{(1)}(\theta_*,b_*),\qquad Z_\beta^{(1)}(\lambda\theta_*,\lambda b_*)=\lambda Z_\beta^{(1)}(\theta_*,b_*),$$

$$W_\beta^{(2)}(\lambda\theta_*,\lambda b_*)=\lambda^2W_\beta^{(2)}(\theta_*,b_*).\qquad\square$$

**Proof of Theorem 2.** Let us fix a value of the parameter $\alpha$ and consider the solution of the Hamilton equations with Hamiltonian $H^{\mathrm{E}}$ defined by (3.1) and the initial conditions

$$t = x = y = z = w = 0, \qquad p_x = \cos\theta, \qquad p_y = \sin\theta, \qquad p_z = c, \qquad p_w = \alpha \tag{5.5}$$

for small $\theta$ and $c$. This solution is approximated up to $O(r^3)$ by the solution (2.2) with the initial conditions (5.2).

Indeed, if $\theta = c = 0$, then the corresponding trajectory $x = t$, $y = 0$, $z = 0$, $w = 0$, $p_x = 1$, $p_y = 0$, $p_z = 0$, $p_w = \alpha$ is a solution of the Hamilton equations with either Hamiltonian, $H^{\mathrm{E}}$ and $H$. (The latter Hamiltonian is defined by (5.1).) Along this trajectory we have $P \equiv 1$ and $Q \equiv 0$, and at all such points the Hamiltonians $H^{\mathrm{E}}$ and $H$ coincide with each other together with their derivatives up to the third order inclusive, since the circle and ellipse (bounding the sets of admissible velocities of the control systems (1.1) and (2.1), respectively) have the same second and third derivatives at the tangency point. Hence, the right-hand sides of the Hamilton equations coincide with each other together with their derivatives up to the second order inclusive. The distance between the initial conditions (5.5) and (5.2) is an infinitesimal $O(r^3)$.

Now, let us write the Hamilton equations with Hamiltonian $H$, this time with the independent variable $t$:

$$\frac{dx}{dt} = \frac{1}{1+Q^2/2}, \qquad \frac{dy}{dt} = \frac{Q}{1+Q^2/2}, \qquad \frac{dz}{dt} = \frac{-xQ/2+y/2}{1+Q^2/2}, \qquad \frac{dw}{dt} = \frac{y^2/2}{1+Q^2/2},$$
$$\frac{dp_x}{dt} = \frac{p_zQ/2}{1+Q^2/2}, \qquad \frac{dp_y}{dt} = \frac{-(p_z/2+p_wy)}{1+Q^2/2}, \qquad \frac{dp_z}{dt} = 0, \qquad \frac{dp_w}{dt} = 0.$$

Up to $O(r^3)$, we obtain

$$\frac{dx}{dt} = 1 - \frac{Q^2}{2}, \qquad \frac{dy}{dt} = Q, \qquad \frac{dz}{dt} = -\frac{tQ}{2} + \frac{y}{2}, \qquad \frac{dw}{dt} = \frac{y^2}{2},$$
$$\frac{dp_x}{dt} = \frac{p_zQ}{2}, \qquad \frac{dp_y}{dt} = -\Big(\frac{p_z}{2} + p_wy\Big), \qquad \frac{dp_z}{dt} = 0, \qquad \frac{dp_w}{dt} = 0,$$

since $x = t + O(r^2)$ due to the invariance under the involution (3.2). Using the solution (2.2) of the Hamilton equations with Hamiltonian $H$ given in the proof of Theorem 1, we obtain

$$x = t - tT^{(2)}_{\alpha t^2}(\theta, ct), \qquad y = tY^{(1)}_{\alpha t^2}(\theta, ct), \qquad z = t^2Z^{(1)}_{\alpha t^2}(\theta, ct), \qquad w = t^3W^{(2)}_{\alpha t^2}(\theta, ct).$$

For $t = 1$, we obtain the asymptotics of Theorem 2 up to $O(r^3)$. For the coordinates $x$ and $w$, the accuracy of the above expansions increases to $O(r^4)$ since they are even with respect to the substitution $(\theta, c) \mapsto -(\theta, c)$, which follows from the invariance under the involution (3.2). □

**Proof of Theorem 3.** Due to the invariance with respect to the quasihomogeneous transformations (1.3), it suffices to prove Theorem 3 for $\tau = 1$. To this end, we apply the already proved Theorem 2.

Let us fix a point $(y_*, z_*, w_*)$ on the surface $\mathcal{F}$ defined by equations (2.5). Suppose that $\theta_*$ and $c_*$ satisfy the conditions

$$T^{(2)}_\alpha(\theta_*, c_*) = 1, \qquad Y^{(1)}_\alpha(\theta_*, c_*) = y_*, \qquad Z^{(1)}_\alpha(\theta_*, c_*) = z_*, \qquad W^{(2)}_\alpha(\theta_*, c_*) = w_*. \tag{5.6}$$

(Such numbers certainly exist since the functions under consideration are homogeneous.) By Theorem 2, we have

$$X_\alpha(\lambda\theta_*, \lambda c_*) = 1 - T^{(2)}_\alpha(\lambda\theta_*, \lambda c_*) + O(\lambda^4) = 1 - \lambda^2 + O(\lambda^4)$$

as $\lambda \to 0+$ in view of (5.6) and the homogeneity of $T^{(2)}_\alpha$. Therefore, for small $\varepsilon > 0$, the equation

$$X_\alpha(\lambda\theta_*, \lambda c_*) = 1 - \varepsilon$$

has a solution $\lambda_\varepsilon = \sqrt{\varepsilon}(1 + O(\varepsilon))$ as $\varepsilon \to 0+$. Indeed, if $\lambda_\varepsilon^2 + O(\lambda_\varepsilon^4) = \varepsilon$, then $\lambda_\varepsilon^2 = \varepsilon + O(\varepsilon^2)$.

Now, from Theorem 2 we obtain

$$y_\varepsilon = Y_\alpha(\lambda_\varepsilon\theta_*, \lambda_\varepsilon c_*) = Y^{(1)}_\alpha(\lambda_\varepsilon\theta_*, \lambda_\varepsilon c_*) + O(\lambda_\varepsilon^3) = \lambda_\varepsilon Y^{(1)}_\alpha(\theta_*, c_*) + O(\lambda_\varepsilon^3) = \sqrt{\varepsilon}\big(y_* + O(\varepsilon)\big),$$

$$z_\varepsilon = Z_\alpha(\lambda_\varepsilon\theta_*, \lambda_\varepsilon c_*) = Z^{(1)}_\alpha(\lambda_\varepsilon\theta_*, \lambda_\varepsilon c_*) + O(\lambda_\varepsilon^3) = \lambda_\varepsilon Z^1_\alpha(\theta_*, c_*) + O(\lambda_\varepsilon^3) = \sqrt{\varepsilon}\big(z_* + O(\varepsilon)\big),$$

$$w_\varepsilon = W_\alpha(\lambda_\varepsilon\theta_*, \lambda_\varepsilon c_*) = W^{(2)}_\alpha(\lambda_\varepsilon\theta_*, \lambda_\varepsilon c_*) + O(\lambda_\varepsilon^4) = \lambda_\varepsilon^2 W^2_\alpha(\theta_*, c_*) + O(\lambda_\varepsilon^4) = \varepsilon\big(w_* + O(\varepsilon)\big).$$

Thus, the point $(y_\varepsilon, z_\varepsilon, w_\varepsilon)$ lies on the cross-section $x = 1 - \varepsilon$ of the Engel front at time 1, and

$$\lim_{\varepsilon\to 0+}\left(\frac{y_\varepsilon}{\sqrt{\varepsilon}}, \frac{z_\varepsilon}{\sqrt{\varepsilon}}, \frac{w_\varepsilon}{\varepsilon}\right) = (y_*, z_*, w_*) \in \mathcal{F}.$$

Therefore, $\mathcal{F}^{\mathrm{E}} \supset \mathcal{F}$. $\square$

## ACKNOWLEDGMENTS

I am grateful to L. V. Lokutsievskiy, A. O. Remizov, Yu. L. Sachkov, and the anonymous referees, whose help in various forms was very useful to me when I worked on the article.

## OPEN ACCESS



## REFERENCES

1. A. A. Agrachev, "Exponential mappings for contact sub-Riemannian structures," J. Dyn. Control Syst. **2** (3), 321–358 (1996).
2. A. Agrachev, B. Bonnard, M. Chyba, and I. Kupka, "Sub-Riemannian sphere in Martinet flat case," ESAIM, Control Optim. Calc. Var. **2**, 377–448 (1997).
3. A. A. Agrachev and Yu. L. Sachkov, *Control Theory from the Geometric Viewpoint* (Springer, Berlin, 2004), Encycl. Math. Sci. **87**.
4. A. A. Ardentov and Yu. L. Sachkov, "Extremal trajectories in a nilpotent sub-Riemannian problem on the Engel group," Sb. Math. **202** (11), 1593–1615 (2011) [transl. from Mat. Sb. **202** (11), 31–54 (2011)].
5. A. A. Ardentov and Yu. L. Sachkov, "Conjugate points in nilpotent sub-Riemannian problem on the Engel group," J. Math. Sci. **195** (3), 369–390 (2013).
6. A. A. Ardentov and Yu. L. Sachkov, "Cut time in sub-Riemannian problem on Engel group," ESAIM, Control Optim. Calc. Var. **21** (4), 958–988 (2015).
7. A. A. Ardentov and Yu. L. Sachkov, "Maxwell strata and cut locus in the sub-Riemannian problem on the Engel group," Regul. Chaotic Dyn. **22** (8), 909–936 (2017).
8. I. A. Bogaevsky, "Asymptotic behaviour of the sphere and front of a flat sub-Riemannian structure on the Martinet distribution," Sb. Math. **213** (5), 624–640 (2022) [transl. from Mat. Sb. **213** (5), 50–67 (2022)].

9. El-H. Ch. El-Alaoui, J.-P. Gauthier, and I. Kupka, "Small sub-Riemannian balls on $R^3$," J. Dyn. Control Syst. **2** (3), 359–421 (1996).
10. M. Gromov, "Carnot–Carathéodory spaces seen from within," in *Sub-Riemannian Geometry* (Birkhäuser, Basel, 1996), Prog. Math. **144**, pp. 79–323.
11. Yu. L. Sachkov and A. Yu. Popov, "Sub-Riemannian Engel sphere," Dokl. Math. **104** (2), 301–305 (2021) [transl. from Dokl. Ross. Akad. Nauk, Mat. Inform. Prots. Upr. **500**, 97–101 (2021)].
12. A. M. Vershik and V. Ya. Gershkovich, "Nonholonomic dynamical systems, geometry of distributions and variational problems," in *Dynamical Systems VII* (Springer, Berlin, 1994), Encycl. Math. Sci. **16**, pp. 1–81 [transl. from Itogi Nauki Tekh., Ser.: Sovrem. Probl. Mat., Fundam. Napravl. **16**, 5–85 (1989)].

*Translated by I. Nikitin*